A R C H I V E S O F M E T A L L U R G Y A N D M A T E R I A L S
Volume 54 2009 Issue 3

A. BOKOTA*, T. DOMAŃSKI**

MODELLING AND NUMERICAL ANALYSIS OF HARDENING PHENOMENA OF TOOLS STEEL ELEMENTS

MODELOWANIE I ANALIZA NUMERYCZNA ZJAWISK HARTOWANIA ELEMENTÓW ZE STALI NARZĘDZIOWYCH

This research the complex model of hardening of tool steel was shown. Thermal phenomena, phase transformations and mechanical phenomena were taken into considerations.

In the modelling of thermal phenomena the heat transfer equations has been solved by Finite Elements Method by Petrov-Galerkin formulations. The possibility of thermal phenomena analysing of feed hardening has been obtained in this way. The diagrams of continuous heating (CHT) and continuous cooling (CCT) of considered steel are used in the model of phase transformations. Phase altered fractions during the continuous heating (austenite) are obtained in the model by formula Johnson-Mehl and Avrami and modified equation Koistinen and Marburger. The fractions ferrite, pearlite or bainite, in the process of cooling, are marked in the model by formula Johnson-Mehl and Avrami. The forming fraction of martensite is identified by Koistinen and Marburger equation and modified Koistinen and Marburger equation. The stresses and strains fields are obtained from solutions by FEM equilibrium equations in rate form. Thermophysical values in the constitutive relations are depended upon both the temperature and the phase content. The Huber-Misses condition with the isotropic strengthening for the creation of plastic strains is used. However the Leblond model to determine transformations plasticity was applied. The numerical analysis of thermal fields, phase fractions, stresses and strain associated deep hardening and superficial hardening of elements made of tool steel were done.

Praca przedstawia kompleksowy model hartowania stali narzędziowej. W rozważaniach uwzględniono zjawiska termiczne, przemiany fazowej i zjawiska mechaniczne.

W modelowaniu zjawisk cieplnych równanie przewodnictwa rozwiązano metodą elementów skończonych w sformułowaniu Petrova-Galerkina. Istnieje zatem możliwość analizowania zjawisk hartowania posuwowego.

W modelowaniu przemian fazowych wykorzystano wykresy ciągłego nagrzewania CTPa i ciągłego chłodzenia CTPc rozważanej stali. Ułamek fazy przemienionej podczas ciągłego nagrzewania (austenit) wyznaczono w modelu równaniem Johnsona-Mehla i Avramiego oraz zmodyfikowanym równaniem Koistinena i Marburgera. Ułamek ferrytu, perlitu lub bainitu, w procesie chłodzenia, wyznacza się równaniem Johnsona-Mehla i Avramiego. Ułamek martenzytu wyznaczany jest równaniem Koistinena i Marburgera oraz zmodyfikowanym równaniem Koistinena i Marburgera. Pola naprężeń i odkształceń otrzymano z rozwiązania metodą elementów skończonych równań równowagi w formie prędkościowej. Wielkości termofizyczne i związki konstytutywne uzależniono zarówno od temperatury jak i od składu fazowego. Do wyznaczenia odkształceń plastycznych wykorzystano warunek plastyczności Hubera-Misessa ze wzmocnieniem izotopowym. Do wyznaczenia odkształceń transformacyujnych zastosowano model Leblonda. Przeprowadzono analizę numeryczną pól temperatury, przemian fazowych, naprężeń i odkształceń towarzyszących głębokiemu hartowaniu oraz przypowierzchniowemu elementów wykonanych ze stali narzędziowej.

1. Introduction

Heat treatment is a technological process, in which thermal phenomena, phase transformations and mechanical phenomena are dominant. Models, which describe processes mentioned above, do not take into consideration many important aspects [1-6]. As a result of the complexity of phenomenon of heat treatment process, there are many mathematical and numerical difficulties in its modelling. For this reason there is no model which would include phenomenon accompanying heat treatment, and therein and hardening.

The correct prediction of the final proprieties is possible after defining the type and the property of the nascent microstructure of the steel-element in the process of heating, and then the cooling treated thermally.

* INSTITUTE OF COMPUTER AND INFORMATION SCIENCES
** INSTITUTE OF MECHANICS AND MACHINE DESIGN, CZESTOCHOWA UNIVERSITY OF TECHNOLOGY, 42-200 CZĘSTOCHOWA, 73 DĄBROWSKI STR., POLAND

To achieve this, it is necessary to establish equations describing temperature fields, phase transformations in the solid state, as well as strains and stresses generated during the heat treatment [1,6-9].

Representant of mechanical phenomenon in process of heat treatment are mainly stress, and their determination is depend on accuracy computing temperature fields and from kinetics of phase transformations in solid state. The kinetics of phase transformations has significant impact on temporary stresses and then on residual stresses [1,6,8-11]. Numerical simulations of steel hardening process need therefore to include thermal strains, plastic, and structural strains and transformations plasticity in the model of heat treatment [9,12,13].

The last decade showed strong evolution of numerical methods in order to in a greater or smaller extent design processes of heat-treatment. Every paper dealing with this topic should contain thermal, microstructural and stress analysis. To implement this type of algorithms one usually applies the FEM, which makes it possible to take into account both nonlinearities and inhomogeneity of thermally processed material [2,4,7-9,14]. Special emphasis put on the development of this branch of numerical methods is inspired by the industry, which demands tools improving heat-treatment processes because of modern technologies and costs reduction trends.

2. Temperature felds and phase transformations

In the modelling of the heat phenomena, convection effects are in many cases significant and cannot be skipped in the conductivity equation. The arguments of the wanted field of the temperature are then space coordinates (Euler coordinates). This approach is comfortable when refers problems of the heat flow in moving objects, or thermal load generated is moving sources of the warmth [7,11,14].

Fields of the temperature determined from equation solution of the transient heat flow with the convection term:

$$\mathrm{div}\left(\lambda \mathrm{grad}\left(T\right)\right) - C\left(\frac{\partial T}{\partial t} + \mathbf{v}\cdot \mathrm{grad}\left(T\right)\right) = -q^{v} \tag{2.1}$$

where $\lambda = \lambda(T)$ is the heat conductivity coefficient, $C = C(T)$ is an effective heat capacity, q^v is intensity of internal sources (one takes into account in him heat of phase transformations), $\mathbf{v}$ is a velocity vector of the small parts (points) of the element (object).

Superficial warming is realised in the model with the boundary condition of the Neumann (heat source $\tilde{q}_n$), and superficial heating is modelled with internal sources generating himself eg. during induction heating. The cooling is modelled by a Newton boundary condition with temperature dependent a convection coefficient:

$$-\lambda \left.\frac{\partial T}{\partial n}\right|_{\Gamma} = \tilde{q}_n = \alpha^{T}\left(T\right)\left(T|_{\Gamma} - T_{\infty}\right) \tag{2.2}$$

On the boundary touching with air (the cooling in air) in the Newton condition one founded, that the coefficient of taking over of the heat took into account both the radiation as and the convection [1,14]:

$$\alpha^{*}\left(T\right) = \alpha_0 \sqrt[3]{T|_{\Gamma} - T_{\infty}} \tag{2.3}$$

where α_0 is coefficient of the heat exchange established experimentally [1,14], Γ is surface, from which the heat is taken over, T_∞ is temperature of the cooling medium.

The finite element method in the Petrov-Galerkin formulation is used to solve the problem. The system of equations to numerical solves is in the form [7,14]:

$$\begin{gathered}\left(\beta\left(K_{ij} + V_{ij} + B_{ij}^{N}\right) + M_{ij}\right)T_j^{s+1} = \left(M_{ij} - (1-\beta)\left(K_{ij} + V_{ij}\right)\right)T_j^{s} + \\ +\beta B_{ij}^{N\infty}T_j^{s+1} + (1-\beta)\,B_{ij}^{N}\left(T_j^{s} - {}^{\infty}T_j^{s}\right) + \beta Q_i^{s+1} + (1-\beta)\,Q_i^{s} - \beta\tilde{q}_i^{s+1} + (1-\beta)\,\tilde{q}_i^{s}\end{gathered} \tag{2.4}$$

where coefficient β represents the schema of the integration with respect to time, ($\beta = 1$ – backward schema Euler, $\beta = 3/4$ – schema Petrov-Galerkin, β=2/3 - schema Galerkin, β=1/2 - schema Crank Nicolson, $\beta = 0$ – schema forward Euler) [7,14], symbol "s" signed the time t, however symbol "s+1" – time $t + dt$.

Matrixes and vectors (2.4) are calculated like:

$$\begin{gathered}K_{ij} = \sum_{e=1}^{M} K_{ij}^{e} = \sum_{e=1}^{M}\int_{\Omega^e} \lambda^{e}\frac{\partial w_i(x_\alpha)}{\partial x_\alpha}\frac{d\phi_j(x_\alpha)}{\partial x_\alpha}d\Omega \\ Q_{ij}^{e} = \int_{\Omega^e} w_i\left(x_\alpha\right)\phi_j\left(x_\alpha\right)d\Omega \\ M_{ij} = \frac{1}{\Delta t}\sum_{e=1}^{e=M} M_{ij}^{e} = \frac{1}{\Delta t}\sum_{e=1}^{e=M} C_{ef}^{e}Q_{ij}^{e} \\ V_{ij} = \sum_{e=1}^{M} V_{ij}^{e} = \sum_{e=1}^{M} v_\alpha^{e}C_{ef}^{e}\int_{\Omega^e} w_i\left(x_\alpha\right)\frac{\partial\phi_j(x_\alpha)}{\partial x_\alpha}d\Omega \\ B_{ij}^{e} = \int_{\Gamma^e} w_i\left(x_\alpha\right)\phi_j\left(x_\alpha\right)d\Gamma, \\ B_{ij}^{N} = \sum_{e=1}^{M^B}\alpha^{T}B_{ij}^{e} \\ Q_i = \sum_{e=1}^{M} Q_{ij}^{e}q_j^{v}, \quad \tilde{q}_i = \sum_{e=1}^{M^B} B_{ij}^{e}\tilde{q}_j\end{gathered} \tag{2.5}$$

where K_{ij}^{e}, Q_{ij}^{e} i B_{ij}^{e} are symmetrical matrix of finite elements called: conductivity matrix, internal source and boundary elements matrix (but in B_{ij}^{N} condition boundary Newton considered was), M_{ij}^{e} is symmetrical matrix of heat capacity (bear also the name – matrix of mass), V_{ij}^{e} is convection matrix, M is number of elements, M^{B} is number of boundary elements, $w_i = w_i(x_\alpha)$ are weights functions, $\varphi_i = \varphi_i(x_\alpha)$ are approximations functions [14].

Heat of phase transformations is considered in the term source of the conductivity equation (2.1) and is calculated with the example [7,10,15-17]:

$$q^{v} = \sum_{k} H_{k}^{\eta_k} \dot{\eta}_k \tag{2.6}$$

where $H_{k}^{\eta_k}$ is volumetric heat (enthalpy) k – phase transformations, $\dot{\eta}_k$ is the rate of change k – phase fraction.

The algorithm of the solving of the conductivity equation in the form (2.4) with suitable initial and boundary conditions and his implementation, gives the possibility of the simulation of the temperature distribution both in Lagrange and Euler coordinates. In this second case one provide $\mathbf{v}(x_\alpha, t) = \mathbf{0}$.

The implementation the algorithm of presented above of solution of the conductivity equation with the finite element method lets on the simulation of thermal loads in axisymmetrical and flat elements (problem 2D) and in axisymmetrical disks and spherical elements (problem 1D). In problems 2D the bilinear approximations functions were used for quadrangular elements, however in problems 1D – linear and square functions. In both case, the weight – functions are shift weigh functions, so-called "upwind function" [14].

In the model of phase transformations diagrams of continuous heating (CHT) and cooling (CCT) are used (fig. 1) [8,18].

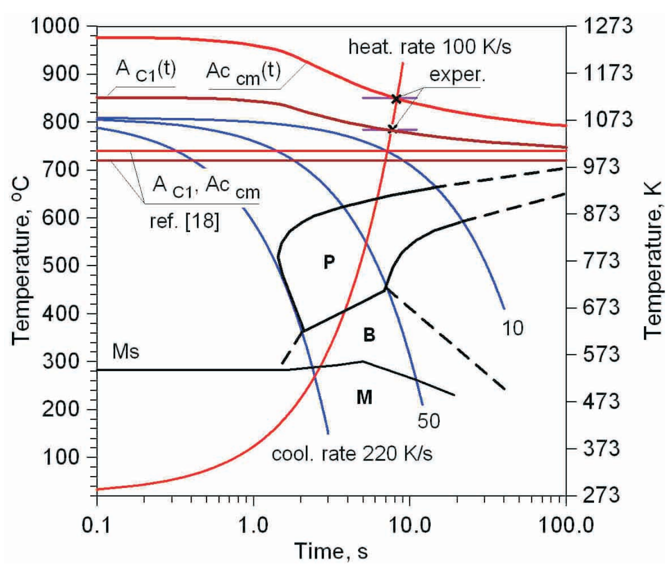

Fig. 1. The Time-Temperature-Transformation graphs (CHT) and (CCT) for steel C80U [7,8]

The phase fraction transformed during continuous heating (austenite) is calculated in the model using the Johnson-Mehl and Avrami formula and modification Koistinen and Marburger formula, for rate heating >100 K/s [9], fractions pearlite or bainite are determined in model by Johnson-Mehl and Avrami formula. The fraction of the martensite formed, is calculated using the Koistinen and Marburger formula [1,8,9]:

$$\begin{gathered}
\underline{\eta}_A (T,t) = 1 - \exp(-b\left(t_s,t_f\right)(t\,(T))^{n(t_s,t_f)}) \\
\underline{\eta}_A (T,t) = 1 - \exp\left(-\tfrac{\ln(\eta_s)}{T_{sA}-T_{fA}}\,(T_{sA} - T)\right), \quad \dot{T} \geqslant 100\,K/s \\
\eta_M (T) = \eta_m \left(1 - \exp\left(-\left(\tfrac{M_s-T}{M_s-M_f}\right)^{m}\right)\right), \quad m = 3.3 \\
\eta_{(\cdot)} (T,t) = \eta_m \left(1 - \exp\left(-b\,(t(T))^{n}\right)\right) \\
\eta_m = \eta_{(\cdot)}^{\%}\underline{\eta}_A \text{ for } \underline{\eta}_A \geqslant \eta_{(\cdot)}^{\%} \text{ and } \eta_m = \underline{\eta}_A \text{ for } \underline{\eta}_A < \eta_{(\cdot)}^{\%}
\end{gathered} \tag{2.7}$$

where $b(t_s, t_f)$ and $n(t_s, t_f)$ are coefficients calculated assuming the initial fraction (η_s=0.01) and the final fraction (η_f=0.99), $\eta_{(\cdot)}^{\%}$ is maximal phase fraction for established cooling rate estimated with CCT diagrams, $\underline{\eta}_A$ is a fractions of the initial austenite, T_{sA} is temperature start austenite transformations, T_{fA} – final temperature of this transformations [9], m is constant from experiment; for considered steel m = 3.3 if for considered steel the temperature start transformations martensite amount M_s=493 K, and final this transformations is in temperature M_f=173 K [7,18].

The purpose of the dilatometric research was to analyse phase transformations during heating and continuous cooling of steel considered. Dilatometric research was done in the Institute for Ferrous Metallurgy in Gliwice by means of a dilatometer DIL805 produced by Bähr Thermoanalyse GmbH. Results of these simulations and appropriate comparisons to the experiment results are presented in pictures [7,8]. The example comparisons are presented the figure 2, the kinetic of transformations established cooling rate are presented on the figure 3 (see [8]).

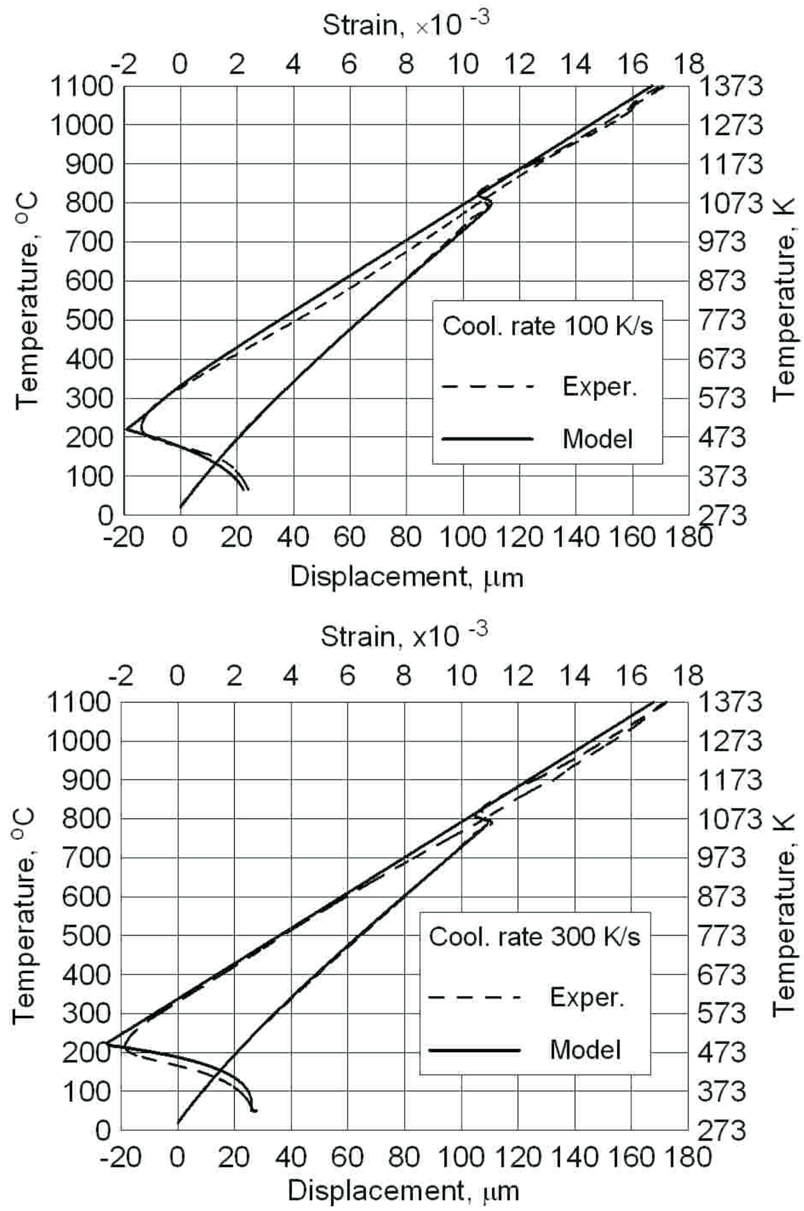

Fig. 2. Experimental and simulated dilatometric curves (see [8])

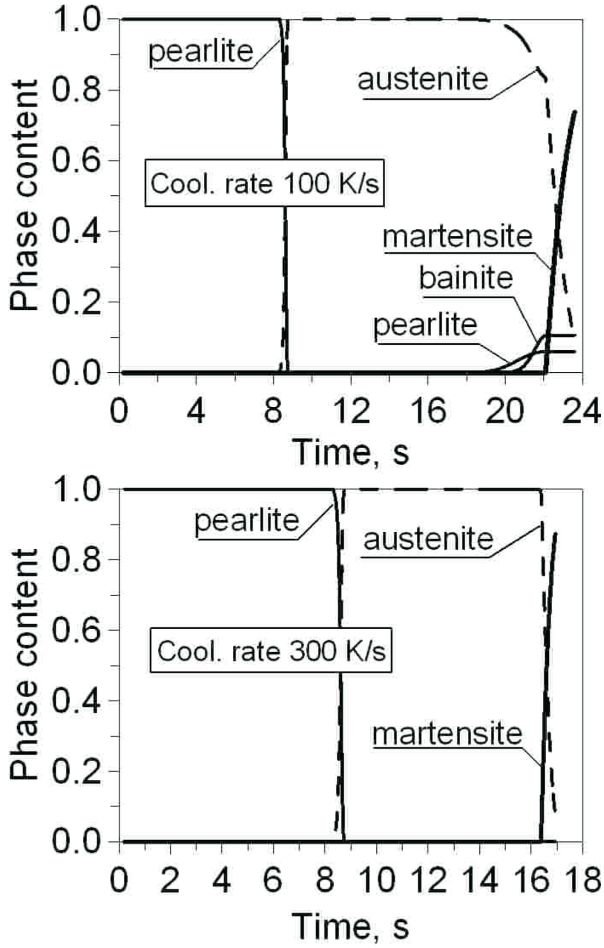

Fig. 3. The kinetic of transformations for established cooling rate (see [8])

The coefficient of thermal expand of pearlite structure is for considered depended from temperature (see fig. 2), so approximation of this coefficient to square function was applied [7,8].

Based on comparisons of experimental and simulator dilatometric curves for the considered steel, values of thermal expansion coefficients and isotropic structural strains of each micro-constituents were determined, they equal: 22, 10, 10 and 14.5 ($\times$ 10^{-6}) [1/K] and 1.0, 4.5, 8.3 and 1.5 ($\times$ 10^{-3}) for austenite, bainite, martensite and pearlite, respectively [7,8].

The simulated dilatometric curves were obtained by solving the increment of the isotropic strain in the processes of heating and cooling using the formula:

$$d\varepsilon^{Tph} = \sum\nolimits_{k=1}^{k=5} \left(\alpha_k \eta_k dT - \operatorname{sgn}(dT)\, \varepsilon_k^{ph} d\eta_k\right) \qquad (2.8)$$

where $\alpha_k = \alpha_k(T)$ are thermal expansion coefficients of: austenite, bainite, ferrite, martensite and pearlite, $\varepsilon_k^{ph} = \varepsilon_k^{ph}(T)$ is an isotropic strain accompanying the conversion of the initial structure into austenite, austenite into bainite, ferrite or cementite fraction, austenite into martensite or austenite into pearlite respectively, sgn (.) is function of sign. In the group of considered steel (C80U, C90U and C100U) ferrite is not performed, therefore $\eta_3 = d\eta_3 = 0$ [8,18].

3. Stresse and strain filds

The equilibrium equation and constitutive relations are used in rate form [7,8,11,14], i.e.:

$$\operatorname{div}\dot{\boldsymbol{\sigma}}(x_\alpha,\, t) = \mathbf{0}, \;\; \dot{\boldsymbol{\sigma}} = \dot{\boldsymbol{\sigma}}^T, \;\; \dot{\boldsymbol{\sigma}} = \mathbf{D} \circ \dot{\boldsymbol{\varepsilon}}^{\mathrm{e}} + \dot{\mathbf{D}} \circ \boldsymbol{\varepsilon}^{\mathrm{e}} \qquad (3.1)$$

where $\sigma = \sigma(\sigma_{\alpha\beta})$ is stress tensor, $\mathbf{D} = \mathbf{D}(v, E)$ is the tensor of material constants (isotropic materials), v is Poisson ratio, $E = E(T)$ is the Young's modulus dependent on the temperature, however ε^e is tensor elastic strains.

Application equilibrium and constitutive equations in rate form permitted change of material property from temperature and phase compositions.

Additivity strains was assumed, i.e. total strains in the around considered points are result of the sum:

$$\varepsilon = \varepsilon^{e} + \varepsilon^{Tph} + \varepsilon^{tp} + \varepsilon^{p} \tag{3.2}$$

where ε^{Tph} are isotope of temperature and structural strains (see. (2.8)), ε^{tp} are transformations plasticity, and ε^{p} are plastic strains.

In order to calculate plastic strains a model of non-isothermal plastic flow with the Huber-Misses plasticity condition and with the isotropic strengthening is used, where the actual effective stress depends on phase composition, temperature and plastic strain [1,7,14]. Flow function (f) have the form:

$$f = \sigma_{ef} - Y\left(T, \eta, \varepsilon^{\mathrm{p}}_{ef}\right) = 0 \tag{3.3}$$

where σ_{ef} is effective stress, $\varepsilon^{\mathrm{p}}_{ef}$ is effective plastic strains, Y is a plasticized stress of material on the phase fraction η in temperature T and effective strains ε^{p}_{ef}:

$$Y\left(T, \eta, \varepsilon^{\mathrm{p}}_{ef}\right) = Y_0\left(T, \eta\right) + Y_H\left(T, \varepsilon^{\mathrm{p}}_{ef}\right) \tag{3.4}$$

where $Y_0 = Y_0(T, \eta)$ is a yield points of material dependent on the temperature and the phase fraction, however $Y_H = Y_H(T, \varepsilon^{p}_{ef})$ is a surplus of the stress resulting from the material hardening.

After considerations (3.4) scalar multiplier of plasticity representation effective plastic strains (ε^{p}_{ef}), solved by formula [7]

$$\dot{\varepsilon}^{p}_{ef} = 2Y \frac{3\mathbf{S} \cdot \left(\left(\mathbf{D} \circ \left(\dot{\varepsilon} - \dot{\varepsilon}^{Tph} - \dot{\varepsilon}^{tp}\right) + \dot{\mathbf{D}} \circ \varepsilon^{\mathrm{e}}\right)\right) - 2Y\left(\kappa^{T}\dot{T} + \sum_k \kappa^{\eta}_{k}\dot{\eta}_k\right)}{9\mathbf{S} \cdot (\mathbf{D} \circ \mathbf{S}) + 4\kappa^{Y}Y^2} \tag{3.5}$$

where $\mathbf{S}$ is the deviator of stress tensor, $\kappa^{Y} = \kappa^{Y}(T, \varepsilon^{p}_{ef})$ is the hardening modulus, $\kappa^{T} = \kappa^{T}(T, \eta, \varepsilon^{p}_{ef})$ is the thermal softening modulus, $\kappa^{\eta}_{k} = \kappa^{\eta}_{k}(T, \varepsilon^{p}_{ef})$ is the modulus of structural softening or hardening [2,3,5].

Can we remark, that rate of effective plastic strain ($\dot{\varepsilon}^{p}_{ef}$) describe (3.5) is depend from value surplus stress, thermophysical gradient of values and of kind output materials structure.

Individual modules are determined following:

$$\begin{aligned}
\kappa^{Y} &= \frac{\partial Y}{\partial \varepsilon^{p}_{ef}} = \frac{\partial Y_H\left(T, \eta, \varepsilon^{p}_{ef}\right)}{\partial \varepsilon^{p}_{ef}} \\
\kappa^{T} &= \frac{\partial Y}{\partial T} = \frac{\partial Y_0(T, \eta)}{\partial T} + \frac{\partial Y_H\left(T, \eta, \varepsilon^{p}_{ef}\right)}{\partial T} \\
\kappa^{\eta}_{k} &= \frac{\partial Y}{\partial \eta_k} = \frac{\partial Y_0(T, \eta)}{\partial \eta_k} + \frac{\partial Y_H\left(T, \eta, \varepsilon^{p}_{ef}\right)}{\partial \eta_k}
\end{aligned} \tag{3.6}$$

The accessible thermophysical values obtained from experiment are Young's modulus $E = E(T, \eta)$ and tangential modulus $E_t = E_t(T, \eta)$. Take advantage of unaxial curves tension or compression, and make use of strains additivity, solved hardening modulus (κ^{Y}), the thermal softening modulus (κ^{T}) and the hardening modulus or structural softening (κ^{η}_{k})[7].

3.1. Transformations plasticity

Numeric simulations of process heat treatment of steel require taking into consideration in models of transformation plasticity. This phenomenon is a reason of irregular, plastic flow metals, which appears during the phase transformations in solid state, especially during transformation austenit to martensit (A→M) cooling iron. In the literature there two different mechanisms, one which has been proposed by Greenwood and Johnson and second by Magge [8,12,13]. In the interpretation of Greenwood-Johnson the transformation plasticity is microplasticity which appear in weaker austenite phase of has caused by difference of volumetric between phases. Magee's interpretation (fundamentally for martensitic transformations), this is the result of change in the orientation of grain martensite which have been newly formed by external load. Priorities of these mechanisms depend on materials and of kind of transformations. Greenwood-Johnson mechanism is priority in diffusivity transformations, and also in bainitic and martensitic transformations when big difference volumetric between phases is.

In this work Leblond's model has been used to estimate transformations plasticity [12]. In the literature there are some other models estimations transformations plasticity (comp. [4,13,19]). However, Leblond's model takes into consideration all transformations and it is used by authors working on modelling heat treatment the most frequently.

Using the Leblond model, completed by decreasing functions (1 - η) which has been proposed by the authors of the work [12], transformations plasticity are calculated as following:

$$\dot{\varepsilon}^{\mathrm{tp}} = \begin{cases} 0, & \text{for } \eta_k \leqslant 0.03, \\ -3\sum_{k=2}^{k=5}\left(1 - \eta_k\right)\varepsilon^{ph}_{1k}\frac{\mathbf{S}}{Y_1}\ln\left(\eta_k\right)\dot{\eta}_k, & \text{for } \eta_k > 0.03 \end{cases} \tag{3.7}$$

where $3\varepsilon^{ph}_{1i}$ are volumetric structural strains when the material is transformed from the initial phase "1" into the k-phase, Y_1 is a actual of phase output (in cooling process is austenite).

Current point of plasticity output phase is calculated by formula

$$Y_1 = Y^{0}_{1} + \kappa^{Y_1}\varepsilon^{tp}_{ef} \tag{3.8}$$

where Y_1^0 is a yield points of output phase, κ^{Y_1} is the hardening modulus of materials about austenite structure, and ε_{ef}^{tp} is effective transformations plasticity. Because no existing suitable date, assumption, that $\kappa^{Y_1} = \kappa^{Y}$.

The equations (3.1) are solved by means of the FEM [7,8,14]. The system of equations used for numerical calculation is:

$$[\mathbf{K}]\ \left\{\dot{\mathbf{U}}\right\} = \left(\left\{\dot{\mathbf{R}}\right\} + \left\{\dot{\mathbf{t}}^{Tph}\right\} - \left\{\dot{\mathbf{t}}^{e}\right\}\right) + \left\{\dot{\mathbf{t}}^{ptp}\right\} \tag{3.9}$$

where $\mathbf{K}$ is the element stiffness matrix, $\dot{\mathbf{U}}$ is the vector of nodal displacement, $\dot{\mathbf{R}}$ is the vector of nodal forces resulting from the boundary load and the inertial forces load, $\dot{\mathbf{t}}^{Tph}$ is the vector of nodal forces resulting from thermal strains and structural strains, $\dot{\mathbf{t}}^{e}$ is the vector of nodal forces resulting from the value change of Young's modulus dependent on the temperature, $\dot{\mathbf{t}}^{ptp}$ is the vector of nodal forces resulting from plastic strains and transformation plasticity.

The rate vectors of loads in the brackets are calculated only once in the increment of the load, whereas the vector $\dot{\mathbf{t}}^{ptp}$ is modified in the iterative process [14].

Have marked rate of displacement solved rate stresses to result to gradient of displacement rate. The final displacements, strains and stress are resulting integration with respect to time, from initial $t = t_0$ to actual time t, i.e.

$$\mathbf{U}(x_\alpha, t) = \int_{t_0}^{t} \dot{\mathbf{U}}(x_\alpha, \tau)\, d\tau,\ \ \boldsymbol{\varepsilon}(x_\alpha, t) = \int_{t_0}^{t} \dot{\boldsymbol{\varepsilon}}(x_\alpha, \tau)\, d\tau,\ \ \boldsymbol{\sigma}(x_\alpha, t) = \int_{t_0}^{t} \dot{\boldsymbol{\sigma}}(x_\alpha, \tau)\, d\tau \tag{3.10}$$

Using one step scheme integration's and marked by index "s" time t, however by index "s+1" – time $t^{s+1} + \Delta t^{s+1}$, summation discrete value functions "**f**" obtain from solutions, in following time steps, carry out following:

$$\mathbf{f}\left(x_\alpha, t^{s+1}\right) = \sum_{k=0}^{k=s} \dot{\mathbf{f}}\left(x_\alpha, \Delta t^{k}\right)\Delta t^{k} + \dot{\mathbf{f}}\left(x_\alpha, \Delta t^{s+1}\right)\Delta t^{s+1} \tag{3.11}$$

In interactions process in following "i" steps are solved the system of equations

$$[\mathbf{K}]\left\{\delta^{i}\dot{\mathbf{U}}\right\} = \left\{\delta^{i}\dot{\mathbf{t}}^{\mathbf{ptp}}\right\} \tag{3.12}$$

and updating successively displacements, strains and stresses

$$\mathbf{f}\left(x_\alpha, t^{s+1}\right) = \sum_{k=0}^{k=s} \dot{\mathbf{f}}\left(x_\alpha, \Delta t^{k}\right)\Delta t^{k} + \left(\dot{\mathbf{f}}^{Tph}\left(x_\alpha, \Delta t^{s+1}\right) + \sum\nolimits_{k=1}^{i} \delta^{k}\dot{\mathbf{f}}\right)\Delta t^{s+1} \tag{3.13}$$

4. Examples of calculation

Numerical simulations of hardening of the elements made of the carbon tool steel were performed. The thermophysical coefficients λ and C were assumed as constants: 35 [W/(mK)], and 5.0 $\times 10^6$ [J/(m^{3}K)]. These are the average values calculated on the basis of the data in the work [5]. Because in work was presented feed hardening assumed that the heats of phase transformation are assumed to zero. Heat transfer coefficient assumed constant equal α^T=4000 [W/(m^{2}K)] (cooling in fluid layer [20]) and α_0=30 [W/(m^{2}K$^{-4/3}$)]. The cooling was modelled with the Newton condition. The temperature of the cooling medium equalled T_∞ =300 K.

Young's and tangential modulus (E and E^t) were dependent on temperature, whereas the yield stress (Y) was dependent on temperature and phase composition. Assumed, that Young's and tangential modulus are equal 2×10^5 and 4×10^3 [MPa] (E^t=$2\times10^{-2}E$), yield points 150, 480, 1150 and 300 [MPa] for austenite, bainite, martensite and pearlite, respectively, in the temperature 300 K. In the temperature of solidus Young's modulus and tangential modulus equalled 100 and 10 [MPa], respectively, whereas yield points equalled 5 [MPa]. These values were approximated with the use of square functions (fig. 4) using the following assumptions based on the work [2]. Fig. 4

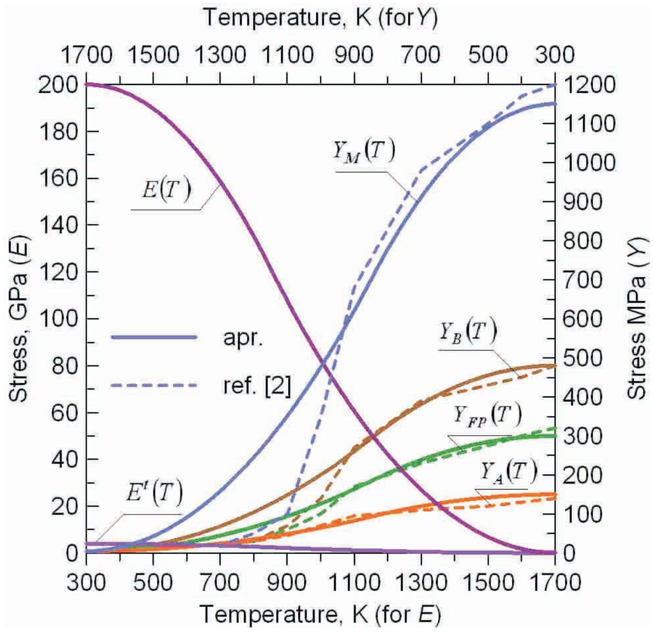

Fig. 4. Diagrams of functions $E(T)$, $E'(T)$ and $Y_0(T,\eta)$

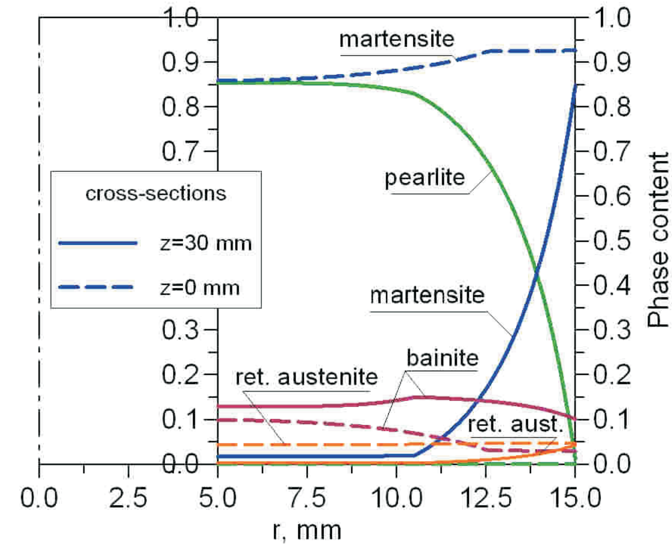

Fig. 6. Hardened zones in the cross sections

4.1. Example 1

The axisymmetrical object with the following size ϕ30×60 mm with mouth ϕ10×mm (fig. 5) underwent hardening simulation. After heating it had an even temperature equalling 1150 K, and the output microstructure was austenite. Fig. 5.

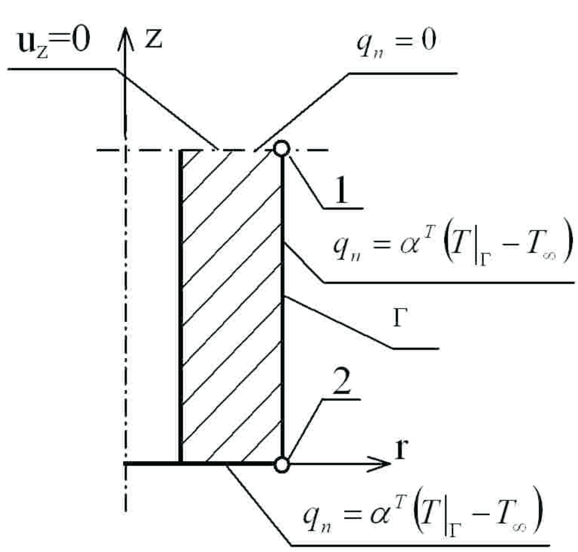

Fig. 5. Scheme of the system and boundary conditions (example 1)

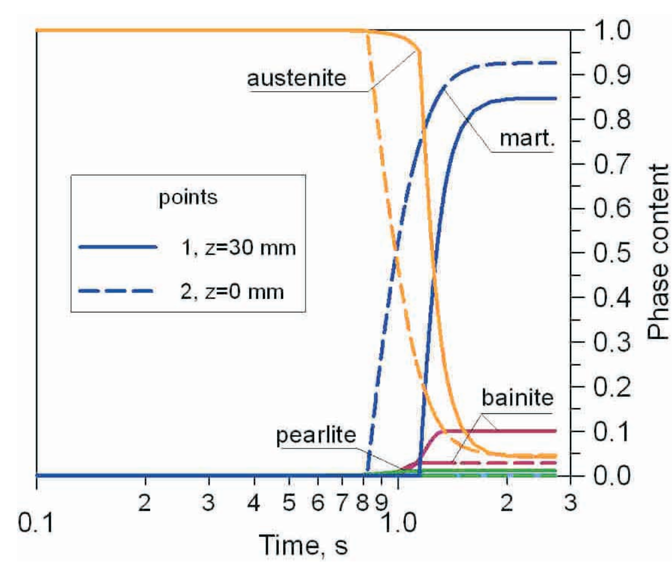

Fig. 7. Kinetic of transformations in the superficial points 1 and 2 of the element (fig. 5)

Hardened zones in the cross sections and the kinetic of transformations in the superficial points 1 and 2 of the element are presented in figures 6 and 7, respectively.

Exemplary residual stresses distributions and plastic strains after hardening, with and without transformation plasticity: ($\varepsilon^{tp} = \mathbf{0}$) and ($\varepsilon^{tp} \neq \mathbf{0}$) are presented in figures 8 and 9, respectively.

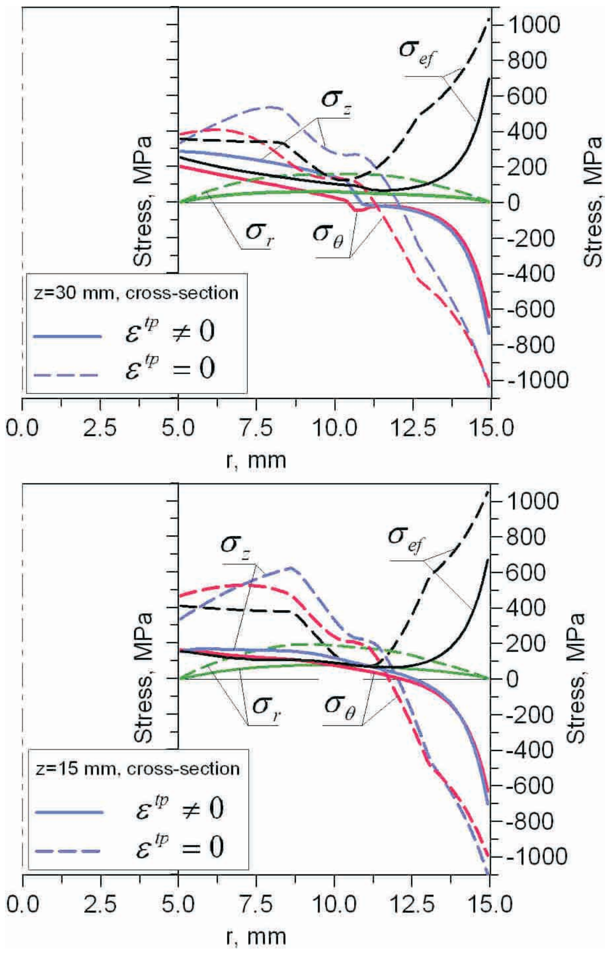

Fig. 8. Residual stresses in the cross sections (fig. 5), without and with considering transformation plasticity

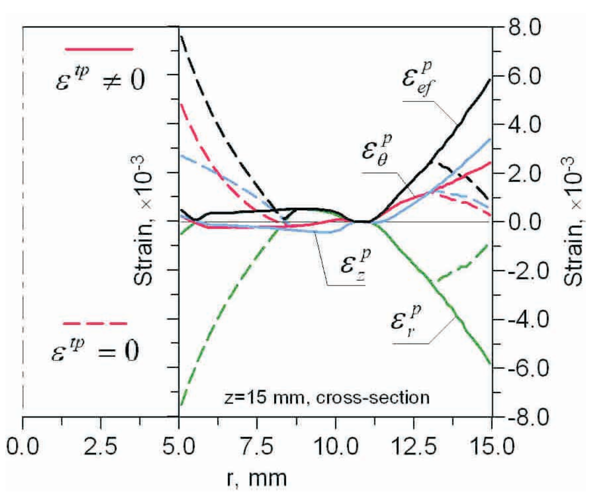

Fig. 9. Plastic strains after hardening, with and without considering transformation plasticity

4.2. Example 2

The axisimmetrical object with the following size ϕ30 mm with mouth ϕ10 mm, made of carbon tool steel C80U. The control region (Euler coordinates) is assumption equal 100 mm. The locations of source, zone intensity cooling and boundary conditions, for conductivity equations (2.1), presented figure 10.

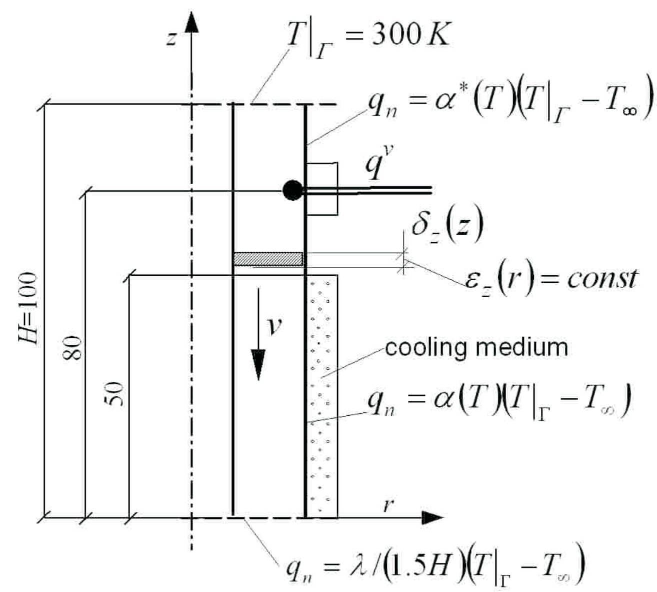

Fig. 10. Scheme of the considered system (example 2)

The heating executed by volumetric source (simulations inductive heating) operate on length 10 mm to depth 1.5 mm. To assume that is depth and hardening superficial. The cooling executed by flux to result from difference of temperature between side surface and medium of cooling (condition Newton) (fig. 10). The initial temperature of hardened model and cooling medium amount 300 K. The thermophysical coefficient accruing in conductivity equations assumed same heavy how in example 1. The solutions investigated for rate of travel v=36 m/h. Power of heating source, to assure maximal of temperature on surface ≈ 1500 K (Fig. 11), equal 4.1 kW. Average density of power equal ≈ 3 [W/mm^3].

The calculations investigate in series system, i.e. the heating simulations to follow to moments of established temperature distributions in control region, and after calculation phase fractions, thermal and structural strains, and then stresses, plastic strains and transformations plasticity.

Because the geometry oh hardened elements is axisymmetrical, to move object in model of mechanical phenomenon of equilibrium equations (3.1), expressed in polar coordinates, reduced to one equations. Problem 1D is solving. To assumed strain plane state, but to modify to, so that obtain reset resultant of force normal ($N|_\Gamma = 0$) in cross-section (Γ). This condition obtain in interactions process to assure conditions [7,11]:

$$\int_0^R \dot{\sigma}_z r dr = 0, \quad \int_0^R \sigma_z r dr = 0 \tag{4.1}$$

After to use constitutive equations on axial stresses ($\dot{\sigma}_z$) [1,7,14]

$$\dot{\sigma}_z = (2\mu + \lambda)\dot{\varepsilon}_z^e + \lambda(\dot{\varepsilon}_r^e + \dot{\varepsilon}_\theta^e) + 2\dot{\mu}\varepsilon_z^e + \dot{\lambda}e^e, \quad e^e = \varepsilon_r^e + \varepsilon_\theta^e + \varepsilon_z^e \tag{4.2}$$

to obtain the formula on average rate of total axial strain:

$$\dot{\varepsilon}_z = \frac{-\int_r \lambda(\dot{\varepsilon}_r^e + \dot{\varepsilon}_\theta^e) r dr - \int_r \left(2\dot{\mu}\varepsilon_z^e + \dot{\lambda}e^e\right) r dr + \int_r (2\mu + \lambda)\left(\dot{\varepsilon}_z^p + \dot{\varepsilon}_z^{Tph} + \dot{\varepsilon}_z^{tp}\right) r dr}{\int_r (2\mu + \lambda) r dr} \tag{4.3}$$

where $\lambda = \lambda(E, \nu)$ $\mu = \mu(E, \nu)$ are constants Lamé [1,14].

The assumption in stress model modified plane state of strain established, that in freely selected disc about differentiable thickness "δ" (see Fig. 10), it can be assumed the loss of deformations of its lateral surface, for the reason of thermal load asymmetrical.

The results of numerical simulations presented in turn figures.

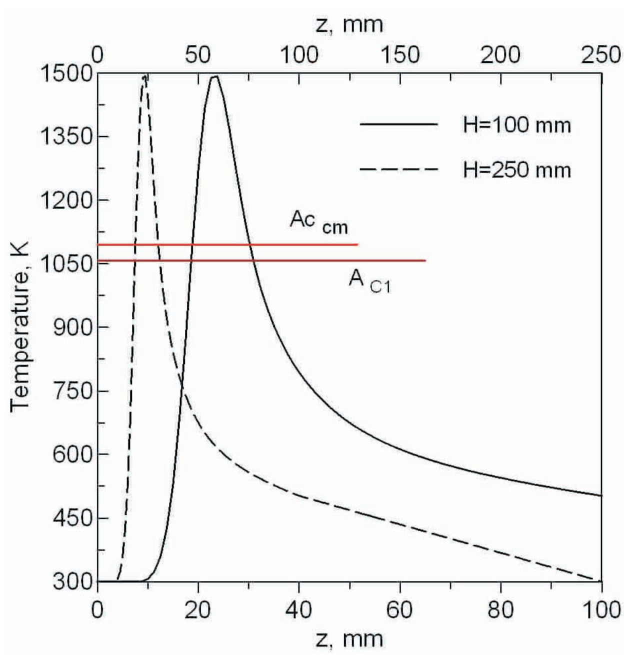

Fig. 11. Temperature distributions on the side surface of the hardening element

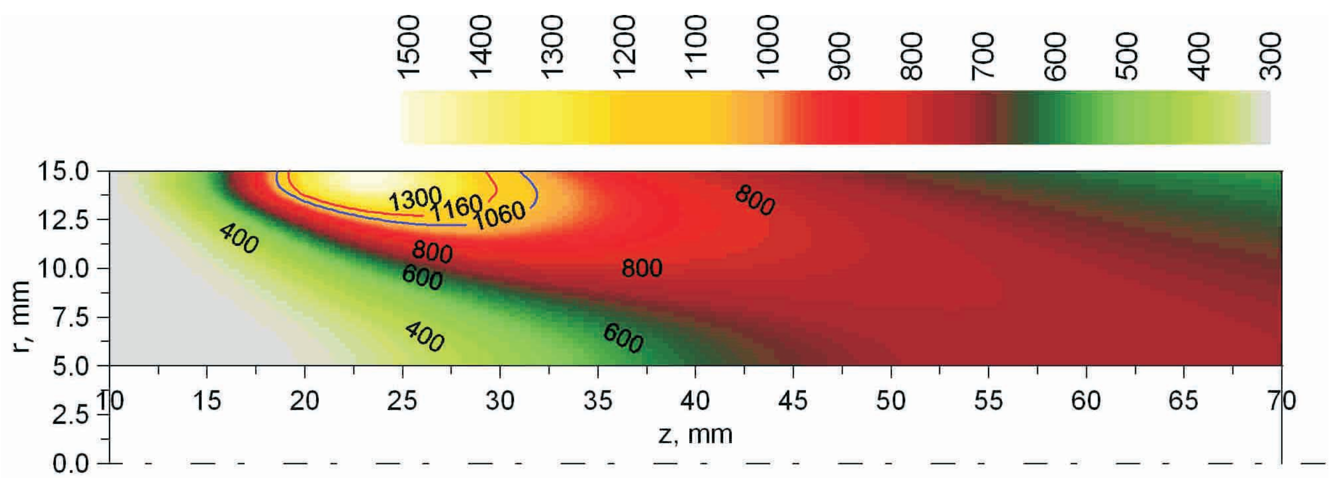

Fig. 12. Temperature distribution in the cross-section of the hardened element

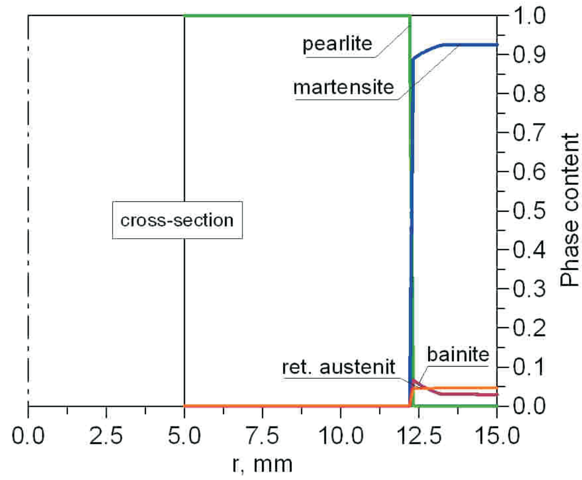

Fig. 13. Hardened zone

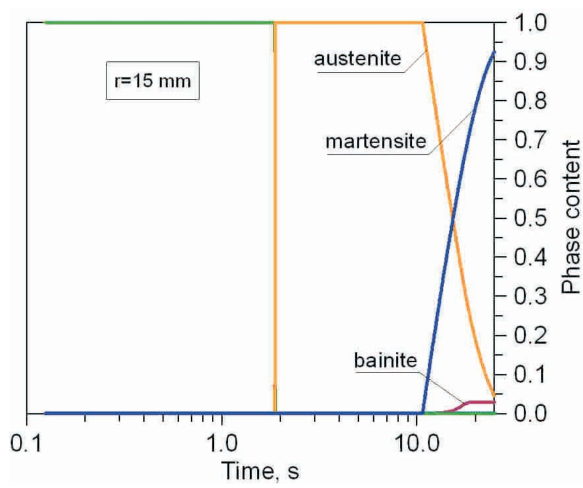

Fig. 14. Kinetic of austenite decay and martensite formation in the superficial point

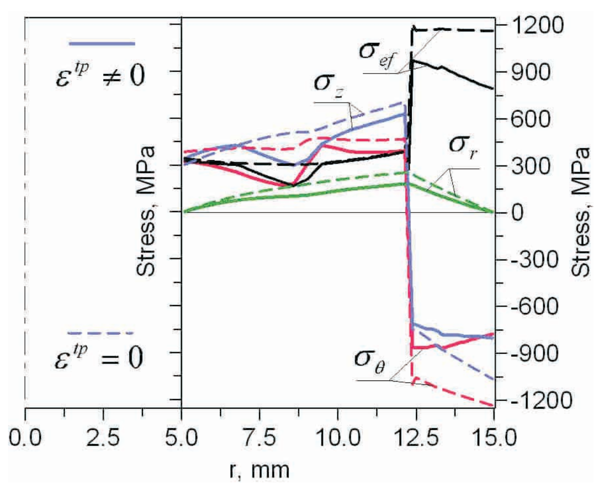

Fig. 15. Residual stresses after hardening, with and without considering transformation plasticity

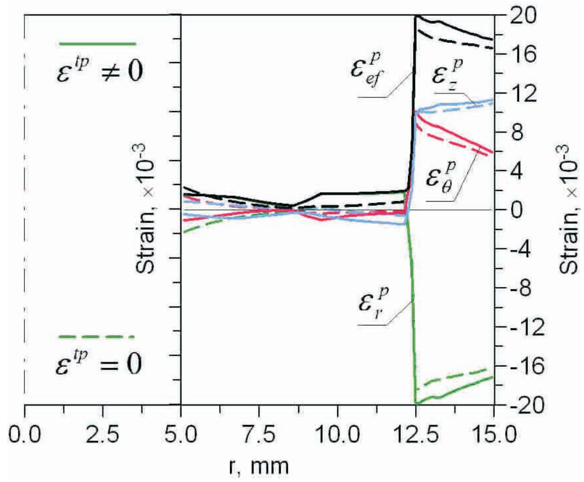

Fig. 16. Plastic strains after hardening, with and without considering transformation plasticity

5. Conclusions

After deep hardening (example 1) the hardened zone is diversified. The mixture of bainite, martensite and pearlite occurs (fig. 6). However nearby the frontal surfaces bainite, martensite and retained austenite occurs. The martensite fraction in frontal layer is very high (~90%) (figs 6 and 7). The internal stress distributions are advantageous (fig. 8). Depositions of negative circumferential and axial stresses is superficial, but deep enough (fig. 8). The meaningful influence on results of calculations of transformations plasticity is observed. It means that in the model taking into consideration the phenomenon of transformation plasticity is not to omit. The results of stress and strain simulations, after such hardening, with and without taking into account transformations plasticity are significantly different (figs. 8 and 9). There is still the problem of reliability of the results, but it could be confirmed with very expensive experiments only.

The plastic strains are in all volume of hardened element, but the obtained distributions are more convincing after taken into account transformations plasticity. The larger strains are in superficial external layer, and not inversely (fig. 9).

Analysing the results obtained in example 2, it was found that in case of feed hardening of element made of tool steel the hardened zone after complex thermal load is comparable to results obtained in the process of inductive hardening [1,14]. The hardened zone with very large martensite fractions is not deep (figs. 13 and 14). The obtaining such hardened zone is the result of suitable thermal load and cooling (figs. 11 and 12). The distributions of stresses after such hardening are advantageous too (compression in surface layer). They are the most different on the limit of hardened zone (fig. 15) in comparison to stress distributions obtained in example 1. The influence on results of transformations plasticity simulation is also observed (figs. 15 and 16) and is smaller than in case of deep hardening (comp. figs 15, 16 and 8, 9).

The presented model of phase fractions calculations in cooling process could by used to simulations of hardening elements made of tool steel C80U, C90U and C100U, because the diagrams CCT for this steel, in terms of shape are similar [18].

Acknowledgements

The research was performed within framework of research project, financed by KBN for years 2007-2009, no. R15 035 02.

REFERENCES

[1] A. J. Fletcher, Thermal Stress and Strain Generation in Heat Treatment, Elsevier, London (1989).

[2] M. Coret, A. Combescure, A mesomodel for the numerical simulation of the multiphasic behavior of materials under anisothermal loading (application to two low-carbon steels), International Journal of Mechanical Sciences **44**, 1947-1963 (2002).

[3] M. Pietrzyk, Through-process modelling of microstructure evolution in hot forming of steels, Journal of Materials Technology **125-126**, 53-62 (2002).

[4] J. Rońda, G. J. Oliver, Consistent thermo-mechanical-metallurgical model of welded steel with unified approach to derivation of phase evolution laws and transformation-induced plasticity, Computer Methods Applied mechanics and engineering **189**, 361-417 (2000).

[5] M. Coret, S. Calloch, A. Combescure, Experimental study of the phase transformation plasticity of 16MND5 low carbon steel induced by proportional and

nonproportional biaxial loading paths. European Journal of Mechanics A/Solids **23**, 823-842 (2004).

[6] W. Piekarska, Numerical analysis of thermomechanical phenomena during laser welding process. The temperature fields, phase transformation and stresses, Wydawnictwo Politechniki Częstochowskiej, Częstochowa (2007), (in polish).

[7] T. Domański, Numerical modelling of surface hardening elements of steel. PhD Thesis, Częstochowa (2005), (in polish).

[8] A. Bokota, T. Domański, Numerical analysis of thermo-mechanical phenomena of hardening process of elements made of carbon steel C80U, Archives of Metallurgy and Materials Issue 2, **52**, 277-288 (2007).

[9] A. Bokota, A. Kulawik, Model and numerical analysis of hardening process phenomena for medium-carbon steel, Archives of Metallurgy and Materials Issue 2, **52**, 337-346 (2007).

[10] L. Huiping, Z. Guoqun, N. Shanting, H. Chuanzhen, FEM simulation of quenching process and experimental verification of simulation results, Material Science and Engineering **A 452-453**, 705-714 (2007).

[11] A. Bokota, W. Piekarska, Modeling of residual stresses in laser welding. The Paton Welding Journal **6**, 19-25 (2008).

[12] L. Taleb, F. Sidoroff, A micromechanical modelling of the Greenwood-Johnson mechanism in transformation induced plasticity, International Journal of Plasticity **19**, 1821-1842 (2003).

[13] M. Cherkaoui, M. Berveiller, H. Sabar, Micromechanical modeling of martensitic transformation induced plasticity (TRIP) in austenitic single crystals, International Journal of Plasticity, **14**, 7, 597-626 (1998).

[14] O. C. Zienkiewicz, R. L. Taylor, The finite element method, Butterworth-Heinemann, Fifth edition, **1,2,3**, (2000).

[15] K. J. Lee, Characteristics of heat generation during transformation in carbon steel. Scripta Materialia **40**, 735-742 (1999).

[16] S. Serejzadeh, Modeling of temperature history and phase transformation during cooling of steel, Journal of Processing Technology **146**, 311-317 (2004).

[17] E. P. Silva, P. M. C. L. Pacheco, M. A. Savi, On the thermo-mechanical coupling in austenite-martensite phase transformation related to the quenching process, International Journal of Solids and Structures **41**, 1139-1155 (2004).

[18] M. Białecki, Characteristic of steels, seria F, tom I, Wydawnictwo Śląsk **108-129**, 155-179 (1987) (in polish).

[19] D. Y. Ju, W. M. Zhang, Y. Zhang, Modeling and experimental verification of martensitic transformation plastic behavior in carbon steel for quenching process, Material Science and Engineering **A 438-440**, 246-250 (2006).

[20] J. Jasiński, Influence of fluidized bed on diffusional processes of saturation of steel surface layer. Seria: Inżynieria Materiałowa Nr 6, Wydawnictwo WIPMiFS, Częstochowa (2003), (in polish).

Received: 20 May 2009.